Assuming that rift deformation mechanisms for 1961–70 were similar to those for 1976–82, we obtain an injection rate of 0.135 m^3/year. This gives a total magma supply rate for 1961 to 1970 of 0.177 km^3/year.
29. D. A. Swanson, *Science* **175**, 169 (1972).
30. Coulomb stress changes are defined as $\Delta S = \Delta\tau - \mu'\Delta\sigma$, where $\Delta\tau$ is the shear stress change on a given failure plane (positive in the direction of fault slip), $\Delta\sigma$ is the change in effective normal stress (positive in compression), and μ' is the effective friction coefficient = 0.35.
31. P. T. Delaney, A. Miklius, T. Árnadóttir, A. T. Okamura, M. Sako, *U.S. Geol. Surv. Open File Rep. 94-567* (1994).
32. We thank the staff of the Hawaiian Volcano Observatory for providing us with the data; P. Okubo and M. Lisowski for useful discussions; P. Okubo for the earthquake summary data; P. Delaney, P. Segall, S. Owen, R. Simpson, and W. Prescott for very useful comments on this manuscript; and P. Segall for the program for computing trilateration station displacements. This research was supported by the U.S. Geological Survey Volcano Hazards Program.

1 March 2000; accepted 17 May 2000

The Chi-Chi Earthquake Sequence: Active, Out-of-Sequence Thrust Faulting in Taiwan

Honn Kao[1] and Wang-Ping Chen[2]

We combined precise focal depths and fault plane solutions of more than 40 events from the 20 September 1999 Chi-Chi earthquake sequence with a synthesis of subsurface geology to show that the dominant structure for generating earthquakes in central Taiwan is a moderately dipping (20° to 30°) thrust fault away from the deformation front. A second, subparallel seismic zone lies about 15 kilometers below the main thrust. These seismic zones differ from previous models, indicating that both the basal decollement and relic normal faults are aseismic.

The Chi-Chi earthquake sequence occurred beneath the fold-and-thrust belt along the western portion of the Taiwan orogen (Fig. 1). This orogen is a consequence of ongoing collision since 5 million years ago (Ma) between the Luzon volcanic arc along the western margin of the Philippine Sea plate and the passive continental margin of southeastern China (Fig. 1) (*1*–*3*).

The Taiwan orogen is a unique natural laboratory for studying collisional processes. First, the orogen is largely exposed above sea level, making it accessible to a wide range of field measurements. Second, the young age of the fold-and-thrust belt provides an opportunity to investigate possible reactivation of structures related to passive margins (*4*, *5*). Third, abundant seismicity can test the critical taper model of mountain building, a concept developed with Taiwan as a typical example (*6*). In central Taiwan, a basal decollement, dipping at a small angle of 5°, was proposed as the controlling geologic structure (*6*).

To this end, the Chi-Chi earthquake sequence is unique. The sequence is well recorded by the Broadband Array in Taiwan for Seismology (BATS), including numerous aftershocks as small as magnitude (M_w) 3.6. A surface rupture of about 80 km in length is well exposed (*7*, *8*). Moreover, the surface rupture is adjacent to regions where subsurface geology has been extensively studied (*9*–*13*).

For the main shock (M_w 7.5) and the three largest aftershocks (M_w 6.2 to 6.4), we used the inversion algorithm of Nábelek (*14*) to determine source parameters. The data are high-quality broadband *P* and *S* waveforms recorded at teleseismic distances by the Global Seismic Network and the French GEOSCOPE Project (Fig. 2). In the inversion, main bursts of seismic moment release are parameterized as subevents, each representing the average properties of a portion of the rupture. One advantage of this representation is its ability to easily accommodate variations in fault plane solutions and focal depths. For the main shock, our results are similar to those of other studies in the overall geometry of faulting, the distribution of slip, and a northward-propagating rupture with increasing amounts of slip (*15*–*17*). Furthermore, our solution resolved a clockwise rotation in the strike of the east-dipping nodal plane toward the northern end of the rupture by nearly 90°, consistent with the observed sharp bend in the trend of the surface rupture (Fig. 1). For the rest of the aftershocks, we carried out inversion of regional broadband waveforms from BATS (*18*) (Web tables 1 and 2) (*19*). On the basis of trends in seismicity and patterns in fault plane solutions, we separated the aftershocks into several groups (Fig. 1). The events in group (a) fall immediately to the east of the subevents during the main shock, forming part of a central cluster trending north-south.

The Chi-Chi sequence produced a surface rupture of 80 km in length along the Chelungpu thrust, which lies to the west of this cluster of numerous aftershocks (*7*). The trend of this cluster follows that of the Chelungpu thrust (Fig. 1). Moreover, the vergence of the Chelungpu fault is westward, consistent with that of all major faults in the epicentral region (*20*) and the fact of high mountains rising to the east. Therefore, the east-dipping nodal plane is likely the fault plane for the main shock and the largest aftershocks in group a, T3 and T4.

A highly unusual aspect of the Chi-Chi sequence is a large difference of over 15 km in focal depths among the aftershocks. This difference is particularly striking between events T3 and T4, whose epicenters are next to each other (Figs. 1 to 3). Yet the two events show a difference of over 8 s in the time interval *sS*-*S*, the differential arrival time between the direct *S*-wave arrival and the reflection off the free surface above the hypocenter, *sS* (Fig. 2).

West of the epicentral region, the foothills and the foreland basin of the orogen were explored for hydrocarbon. We synthesized seismic reflection profiles, borehole data, and detailed surface mapping to provide geologic context for understanding earthquake-generating (seismogenic) structures (Fig. 3).

In the foreland, the most obvious structural feature is the Pakuashan anticline (Fig. 3), an elongated, north-south–trending topographic high (Fig. 1). The subsurface geology of this structure is well constrained by seismic reflection profiles and two boreholes (Fig. 3) (*9*–*11*). In particular, Chen (*9*) interpreted the Pakuashan fault as a ramp thrust, postdating the infill of the foreland basin of Pleistocene age (~1 Ma) (*20*). Another important feature beneath the Pakuashan anticline is a high-angle hinge fault (Fig. 3), produced during the opening of the South China Sea (*21*). The Pakuashan thrust appears to postdate any reverse slip along the hinge fault (Fig. 3), and the deformation front of the Taiwan orogen has reached farther to the west of the Pakuashan thrust.

Surface rupture of the Chi-Chi sequence, the Chelungpu fault, marks the eastern boundary of the foreland basin (*10*–*13*). Near the surface, all strata between the Chelungpu and the Shaungtung thrusts are monoclines dipping to the east at 20° to 30° (*10*, *13*). The Chelungpu thrust has a similar geometry down to a depth of ~5 km (*10*). This geometry is constrained by numerous seismic reflection profiles, most of which remain proprietary.

Although the Chelungpu fault probably

[1]Institute of Earth Sciences, Academia Sinica, Nankang, Taipei, Taiwan 115, Republic of China. [2]Department of Geology and Mid-America Earthquake (MAE) Center, University of Illinois, Urbana, IL 61801, USA.

initiated as a listric thrust (*6*), a planar extension of this thrust from the surface to a depth of about 15 km provides a straightforward explanation for the main rupture of the Chi-Chi sequence. First, an average dip of 25° of the Chelungpu thrust is consistent with the range of apparent dips of the fault plane (20° to 30°) of the largest events (S2 to S4 and T4) (Fig. 3). Second, the centroids of these events cluster around such a planar structure.

At greater depths, the data indicate a second seismogenic zone. The strongest evidence is the difference in depths of about 15 km between the two large aftershocks, T3 and T4 (Fig. 2). The depth of event T3 alone suggests that this event does not belong to the same cluster as events S2 to S5 and T4 (Fig. 3). Furthermore, apparent dips of the east-dipping nodal plane for events T3 and B8 are also close to 25°, suggesting that a planar structure extends up dip from event T3 by about 15 km. We interpret aftershocks B4, B13, and B23 as part of this second, deeper seismic zone.

Overwhelmed by large signals from later subevents, the initiation of the main shock, subevent S1, has large uncertainties in its focal depth. Consequently, one cannot resolve if the rupture nucleated on the main seismogenic zone. Because uncertainties in locating earthquakes are unlikely to be small enough to define a set of exact planes, we see no evidence to propose a more complex seismogenic structure than that depicted in Fig. 3 (*22*). Although seismogenic thrust faulting has been observed down to 30 to 40 km in zones of recent convergence (*23*), our results suggest that such faulting occurs along well-defined structures down to depths of about 30 km.

Because the deformation front of the Taiwan orogen has advanced westward beyond the Pakuashan thrust (Fig. 3) (*24*), the Chi-Chi sequence alone shows that the Chelungpu fault is an active, out-of-sequence thrust—a thrust fault that develops or remains active in the hinterland of a fold-and-thrust belt (*25*, *26*). Moreover, field investigations show that the Chelungpu fault system itself has migrated toward the hinterland (*7*). The configuration of this fault system depicted in Fig. 3 is in marked contrast to previous models of the Taiwan orogen in which either a basal decollement, dipping at a small angle of 5° (*6*), or the reactivation of high-angle (>60° in dip) normal faults is the controlling geologic structure (*4*, *5*).

The second, deeper seismogenic zone during the Chi-Chi sequence also has important implications for seismic hazard. In southwestern Taiwan, moderate-sized earthquakes (up to M_w 6.2) occur at depths of 20 to 25 km (*27*–*29*). If structures associated with the Chi-Chi sequence extend southward, these moderate-sized earthquakes may have occurred on the deeper, secondary seismic zone. However, it is the shallower thrust fault that poses the greatest earthquake hazard.

Indeed, aftershocks in groups (b) and (c) provide indications for the lateral termination of the Chelungpu fault system. To the south, large aftershocks in group (b) show left-lateral slip on northwest-trending nodal planes. The extent of this cluster is nearly 50 km along the same trend (Fig. 1). To the north, aftershocks show an east-northeast trend [group (c)]. Except for event B1, one nodal plane of the other large aftershocks is subparallel to this trend and shows right-lateral slip (Fig. 1). Thus, the main rupture of the Chi-Chi sequence terminated in strike-slip fault zones that accommodate the westward slip of the hanging wall of the Chelungpu fault (Fig. 1).

The relation between the main rupture zone and the rest of the aftershocks is not simple. In general, the compression (*P*) axes of the fault plane solutions show a consistent trend of west-northwest, subparallel to the direction of plate convergence (Fig. 1). The small cluster of events in group (d) may be related to coseismic loading of the footwall of the Chelungpu fault. However, because there is an aseismic region west of group (e), it is not clear if this group is related to the Chi-Chi sequence. Finally, seismicity in group (f) overlaps with the surface expression of a major earthquake in 1906 (M_w 7.1), raising the question of whether out-of-sequence faults also pose a serious seismic hazard for southwestern Taiwan (*30*).

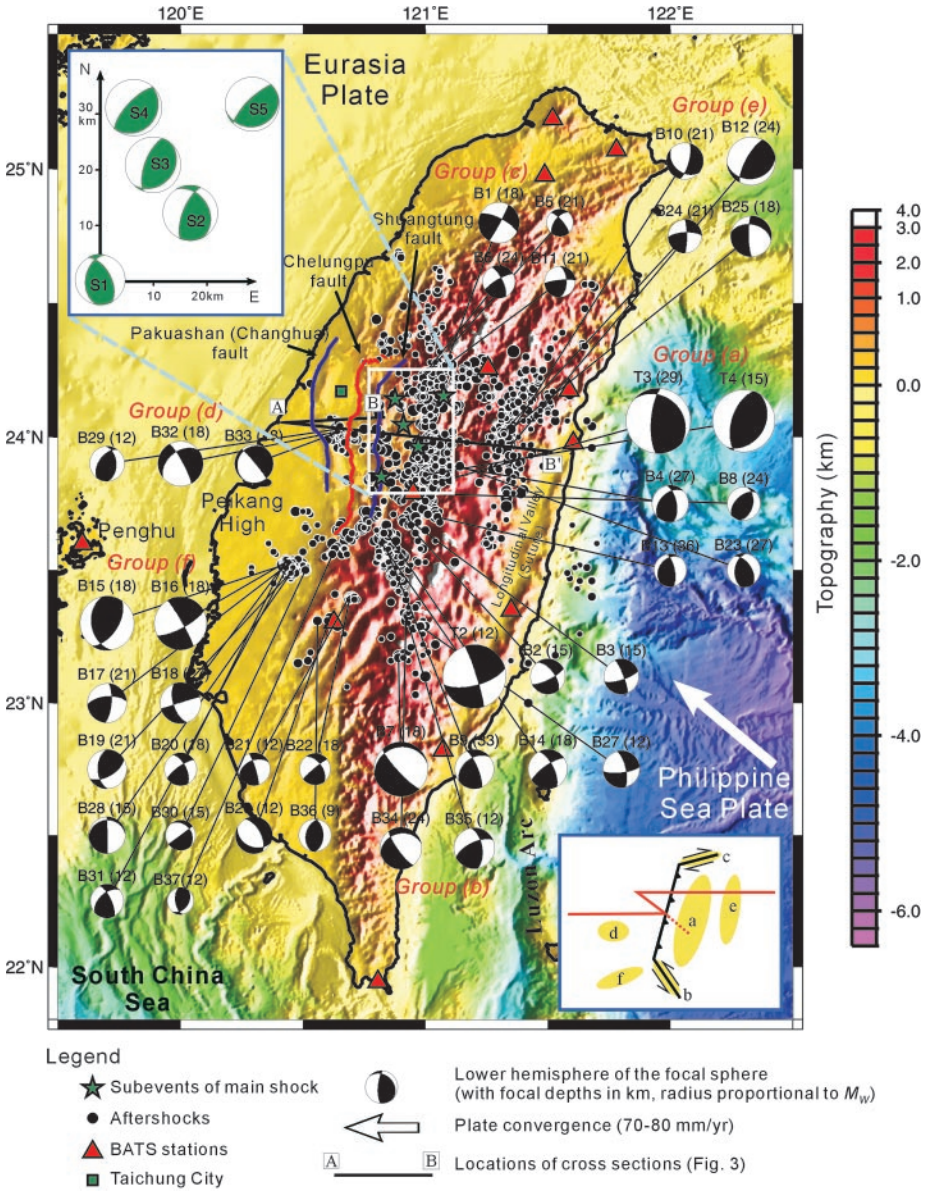

Fig. 1. Map showing epicenters of the Chi-Chi sequence and fault plane solutions (large symbols, in equal-area projection with the compressional quadrants darkened). The lower inset shows the hanging wall of the Chelungpu thrust moved westward, terminating laterally at strike-slip zones.

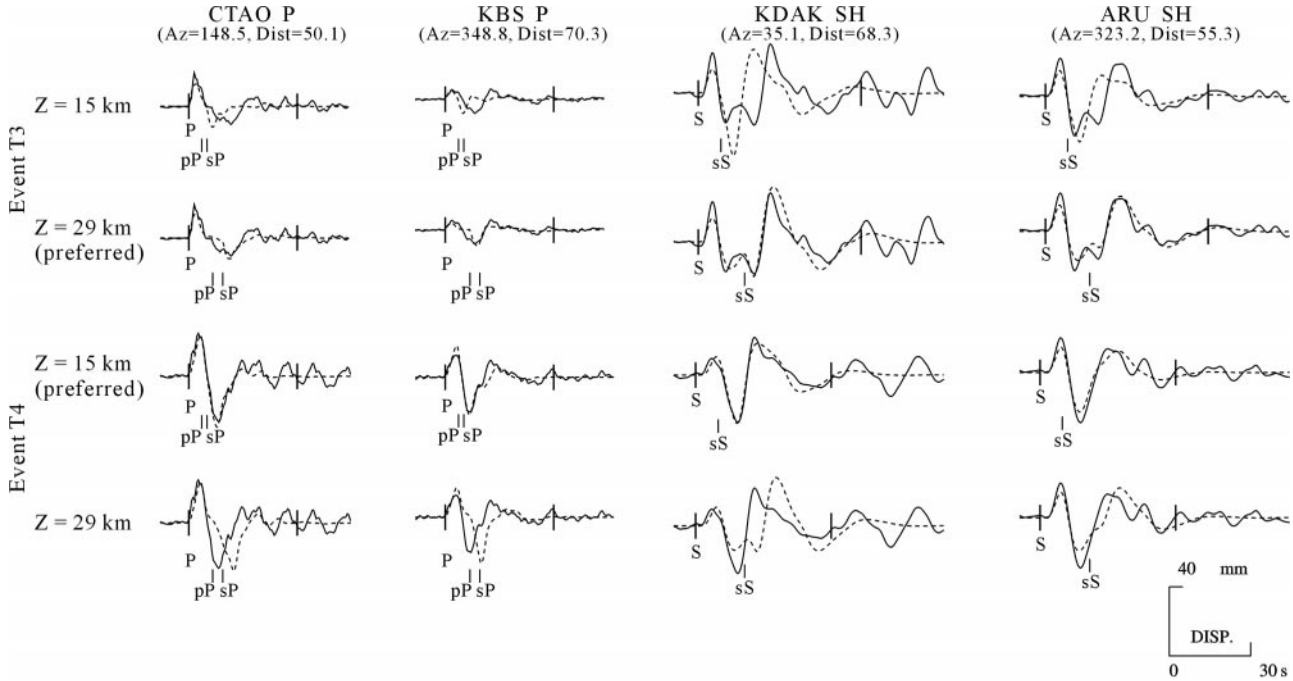

Fig. 2. Examples of observed (solid traces) and synthetic broadband (dashed traces) seismograms illustrating the difference in depth between two large aftershocks T3 and T4. Notice the large time interval between arrivals *sS* and *S* for event T3, indicating a depth of near 30 km. Z, focal depth; Az, azimuth (degrees); Dist, epicentral distance (degrees); and DISP, ground displacement.

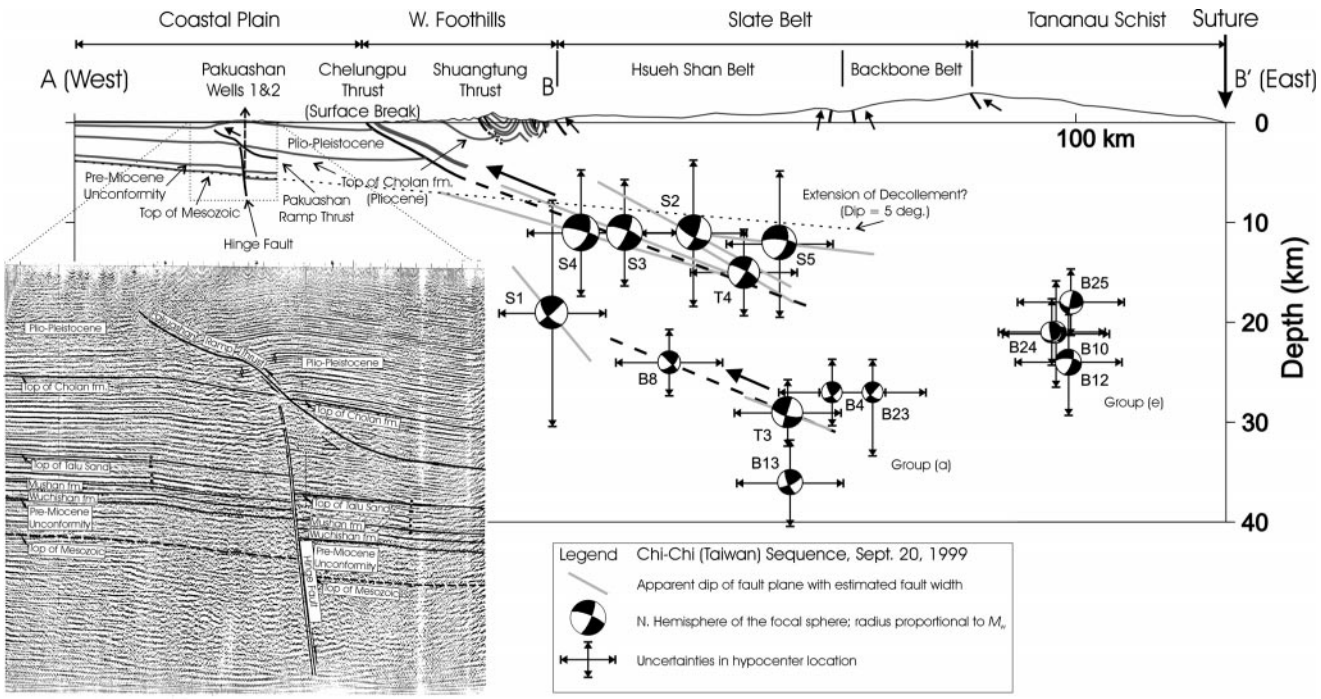

Fig. 3. Cross section of the Taiwan orogen (*31*). The seismic profile (inset, collected along line AB) (*9*, *11*, *12*) is rescaled and projected onto the cross section AB′ (Fig. 1). We assigned an uncertainty of ±5 km to the epicenters, a value approaching the station spacing of the dense local seismic networks (*32*). The active Chelungpu thrust is an out-of-sequence fault, evident from the deformation farther west. A near-planar extension of the Chelungpu thrust explains apparent dips of fault planes and depths for the largest shocks in the Chi-Chi sequence. Another deeper seismic zone is also apparent. Both relic normal faults (e.g., hinge fault in inset) and the basal decollement appear to be aseismic.

References and Notes

1. J. Suppe, *Acta Geol. Taiwan.* **26**, 1 (1988).
2. T. Seno, S. Stein, A. E. Gripp, *J. Geophys. Res.* **98**, 17941 (1993).
3. S.-B. Yu, H.-Y. Chen, L.-C. Kuo, *Tectonophysics* **274**, 41 (1997).
4. Y.-L. Chang, C.-I. Lee, C.-W. Lin, C.-H. Hsu, E.-W. Mao, *Pet. Geol. Taiwan* **30**, 163 (1996).
5. J. Suppe, *Pet. Geol. Taiwan* **20**, 85 (1984).
6. D. Davis, J. Suppe, F. A. Dahlen, *J. Geophys. Res.* **88**, 1153 (1983).
7. Y.-G. Chen *et al.*, in preparation.
8. K.-F. Ma, C.-T. Lee, Y. B. Tsai, T. C. Shin, J. Mori, *Eos* **80**, 605 (1999).
9. J.-S. Chen, *Pet. Geol. Taiwan* **15**, 199 (1978).
10. S. L. Chang, *Pet. Geol. Taiwan* **8**, 21 (1971).
11. H. T. Chiu, *Pet. Geol. Taiwan* **8**, 7 (1971).
12. P.-T. Hsiao, *Pet. Geol. Taiwan* **6**, 209 (1968).

13. S. C. Sun, *Pet. Geol. Taiwan* **4**, 161 (1965).
14. J. L. Nábelek, thesis, Massachusetts Institute of Technology, Cambridge, MA (1984).
15. K.-F. Ma *et al.*, in preparation.
16. C.-H. Chen and Y. Zeng, *Eos* (Fall Meet. Suppl.) **80**, 12 (1999).
17. C.-T. Lee, C.-T. Cheng, S.-K. Hsu, *Eos* (Fall Meet. Suppl.) **80**, 14 (1999).
18. H. Kao, P.-R. Jian, K.-F. Ma, B.-S. Huang, C.-C. Liu, *Geophys. Res. Lett.* **25**, 3619 (1998).
19. Web tables 1 and 2 are available at www.sciencemag.org/feature/data/1049578.shl.
20. J.-C. Lee *et al.*, *Terr. Atmos. Oceanogr.* **7**, 431 (1996).
21. T.-Y. Lee and L. Lawver, *J. Geol. Soc. China* **35**, 353 (1992).
22. P. Molnar and W.-P. Chen [in *Mountain Building Processes*, K. Hsü, Ed. (Academic Press, San Diego, CA, 1982), pp. 41–57] proposed a similar configuration of subparallel seismogenic faults in the Himalayan collision zone. The current study suggests that out-of-sequence thrusts in the Himalaya may also pose a high seismic risk.
23. W.-P. Chen and P. Molnar, *J. Geophys. Res.* **88**, 4183 (1983).
24. S.-C. Fuh, C.-S. Liu, M.-S. Wu, *Pet. Geol. Taiwan* **31**, 43 (1997).
25. C. K. Morely, *Tectonics* **7**, 539 (1988).
26. S. Boyer, in *Structural Geology of Fold and Thrust Belts*, S. Mitra and G. Fisher, Eds. (Johns Hopkins Univ. Press, Baltimore, MD, 1992), pp. 161–188.
27. R. J. Rau and F. T. Wu, *Earth Planet. Sci. Lett.* **133**, 517 (1995).
28. B.-S. Huang, K.-C. Chen, Y. T. Yeh, *J. Geol. Soc. China* **39**, 235 (1996).
29. F. T. Wu, R.-J. Rau, D. Salzberg, *Tectonophysics* **274**, 191 (1997).
30. The critical taper model has also been proposed for this region [J. Suppe, *Mem. Geol. Soc. China* **4**, 67 (1981)] and for northwestern Taiwan [J. Suppe and J. Namson, *Pet. Geol. Taiwan* **16**, 1 (1979)]. For central Taiwan, our speculation is that the presence of the Peikang high east of Penghu, a well-known structural high, impedes the westward advance of the deformation front, causing out-of-sequence slip on the Chelungpu thrust. The Peikang high correlates with the major recess in the overall geometry of the western Taiwan fold-and-thrust belt (Fig. 1).
31. W.-P. Chen, *Mid-America Earthquake Center Rep*. **SG-6B** (2000).
32. T. C. Shin, K. W. Kuo, W. H. K. Lee, T. L. Teng, Y. B. Tsai, *Seismol. Res. Lett.* **71**, 23 (2000).
33. The National Science Council of the Republic of China and the NSF/MAE Center supported this research.

17 February 2000; accepted 17 May 2000

Accommodating Phylogenetic Uncertainty in Evolutionary Studies

John P. Huelsenbeck,[1]* Bruce Rannala,[2] John P. Masly[1]

Many evolutionary studies use comparisons across species to detect evidence of natural selection and to examine the rate of character evolution. Statistical analyses in these studies are usually performed by means of a species phylogeny to accommodate the effects of shared evolutionary history. The phylogeny is usually treated as known without error; this assumption is problematic because inferred phylogenies are subject to both stochastic and systematic errors. We describe methods for accommodating phylogenetic uncertainty in evolutionary studies by means of Bayesian inference. The methods are computationally intensive but general enough to be applied in most comparative evolutionary studies.

The processes of mutation, selection, and genetic drift that underlie evolutionary change operate very slowly in most species. Many questions in evolutionary biology are therefore addressed by comparing molecular, morphological, ecological, or behavioral characteristics among groups of species (*1*). The comparative method, for example, uses comparisons of the states at two or more characters among extant species as a tool for detecting the evidence of adaptation. Correlated change among characters is the footprint of natural selection. Similarly, comparative analyses of DNA sequences have transformed molecular evolutionary studies, indicating evidence of strong purifying selection and, more rarely, evidence for positive selection at the molecular level. Many evolutionary biologists, however, are concerned with much simpler questions than whether characters have changed in a correlated manner. For example, a question commonly asked in comparative evolutionary studies is whether certain traits are capable of rapid evolutionary change and whether they change in a biased manner over evolutionary time. Such studies typically examine the number of times that a trait has been gained and lost over the evolutionary history of a group of related species.

Most evolutionary biologists now recognize that phylogenetic history must be accommodated in comparative analyses. Otherwise, the covariation among characters induced by their common phylogenetic history can compromise a statistical analysis (*2*). Accordingly, the "gold standard" of between-species studies today includes a phylogenetic analysis. However, phylogenies used in comparative studies are typically treated as known (*1*). Although wary of this assumption, in the absence of any clear alternative the usual response of biologists has been to "hedge bets" by performing the analysis with only the well-supported parts of a phylogeny, or with phylogenies obtained by several methods with the implicit assumption that the conclusions of the analysis are well founded if they are robust to the method of phylogenetic inference used. Recent attempts to accommodate phylogenetic uncertainty seek to ascertain the sensitivity of a comparative study to the phylogeny used (*3*) or to average over all possible phylogenies generated by a stochastic model of cladogenesis (*4*). Such approaches do not make efficient use of information about the relative probabilities of potential phylogenies that can be obtained from a sample of DNA sequences. Developing a formal method for dealing with phylogenetic uncertainty in comparative analyses is important for at least two reasons: (i) estimates of phylogeny are subject to both systematic and stochastic errors (*5*, *6*) and (ii) evolutionary biologists often have only a peripheral interest in phylogeny and are more interested in testing evolutionary hypotheses.

Recently developed methods for phylogenetic analysis with molecular data make it possible to perform comparative analyses in such a way that inferences are averaged over all possible trees (*7*, *8*); the character analysis is performed on each tree, and the result is weighted by the posterior probability (*9*) that the tree is correct. For even moderate numbers of species, it is usually not feasible to perform a comparative analysis by considering all possible trees. This ideal can be approximated, however, by sampling trees according to their (posterior) probability given the existing data. We illustrate this idea by asking how many times the horned soldier caste evolved and was lost in aphids (*10*). This question is typical of the type of question asked by many evolutionary biologists. There are two sources of uncertainty in studies of the evolution of a particular character: (i) uncertainty about the phylogenetic tree of the species under study and (ii) uncertainty about the character transformations on that tree. We illustrate two ways in which such uncertainties can be considered. The first approach accommodates uncertainty in the phylogenetic tree by averaging over possible trees weighted according to their posterior probabilities but ignores the inherent

[1]Department of Biology, University of Rochester, Rochester, NY 14627, USA. [2]Department of Medical Genetics, University of Alberta, Edmonton, Alberta T6G 2H7, Canada.

*To whom correspondence should be addressed. E-mail: johnh@brahms.biology.rochester.edu